

Design, Implementation, and Test Flight of a Lightweight Camber Morphing Wing Aircraft

Md Azizul Islam¹, Azizur Rahman², Achintya Kumar Saha³, and Bruce W. Jo⁴
Tennessee Technological University, Cookeville, TN, 38505, USA

Abstract

Inspired by nature and avionic birds, this paper introduces the process of designing, building, and flying a camber-morphing wing unmanned aerial vehicle (UAV). Unlike conventional fixed-wing aircraft that use control surfaces such as flaps and ailerons for flight control, the concept of morphing is a more substantial and conformal shape change that has the advantages of enhanced aerodynamic performances, including longer flight time and range, radar signature, from increased lift (L), reduced drag (D), or improved L/D, lift and drag ratio at a certain angle of attack (AoA) range. Camber is the curvature of the airfoil, and camber morphing is one way to adjust the camber rate or curvature, thereby modifying the flight profile by altering L and D. Numerical analysis of the aerodynamic performance of camber morphing airfoils compared to conventional wings with control surfaces reveals that camber morphing outperforms. In addition, most morphing designs are not conformal but rather employ partial morphing in either the trailing or leading edge of the airfoil. Various studies have demonstrated the effectiveness of camber morphing; however, most research related to morphing focuses on aerodynamic analysis and is primarily conceptual, often existing only in academic papers. The actual system and its performance verification have yet to be fully developed for UAVs, as camber morphing requires specific internal mechanisms that are lightweight and simple and conformally change the camber rate accordingly. This paper presents the detailed design, implementation, performance evaluation, and test flight of the developed, entirely conformal camber morphing wing UAV. The impact of lightweight, reduced noise, and enhanced L/D aerodynamic performance of the designed UAV is introduced in this paper. Its significant contribution lies in the actual and effective implementation of the entire camber morphing, including leading and trailing edges, for various futuristic applications.

Introduction

The term ‘morph’ is from the Greek word “metamorphosis,” as in ‘to change shape and form’ – a biological development process in which forms change [1-4]. In engineering terms, morphing refers to the use of a Smart structure or an approach that utilizes compliant or rigid body mechanisms or materials. The main goal of the morphing is to provide systems with additional functions or features to adapt to external changes [5]. In aerospace or mechanical engineering disciplines, the technologies using morphing concepts refer to any efforts to enhance the sustainability of the aircraft that relates to flight performance, including maneuverability and the flight envelope, by substantially and actively altering aircraft wing shapes, which corresponds to different flight modes and external conditions [6]. Among various techniques to make aircraft more sustainable, morphing focuses on the wing configuration by making substantial shape changes to correspond to optimal flight conditions. However, the physical adoption of morphing structures to large-scale aircraft for real-world operations is challenging due to unguaranteed structural safety [7]. So, the morphing mechanisms are a critical design aspect. Another common approach is to utilize new energy sources, such as hydrogen, batteries, or a combination of both. Recently, new propulsion systems for carbonless emission commercial aircraft have also been considered [8]. The authors in this paper define the scope of the work, focusing on morphing structures applied to low-speed UAVs, specifically on more efficient morphing mechanisms and their applications to real-scale UAVs, ultimately leading to futuristic aircraft designs [8, 9].

While conventional aircraft morph wing shapes in fixed boundaries using discrete and deployable control surfaces such as flaps, ailerons, and rudders, as shown in Fig. 01, morphing wing aircraft in aerospace use an internal morphing mechanism or smart structures, thereby possibly generating more substantial and flexible wing-shaped changes toward near optimal shapes [10-18] corresponding to flight conditions.

¹ Graduate Student, Department of Mechanical Engineering, mislam59@tntech.edu

² Graduate Student, Department of Mechanical Engineering, arahman46@tntech.edu

³ Graduate Student, Department of Mechanical Engineering, AIAA Student Member, aksaha42@tntech.edu

⁴ Associate Professor, Department of Mechanical Engineering, AIAA Member, bjo@tntech.edu

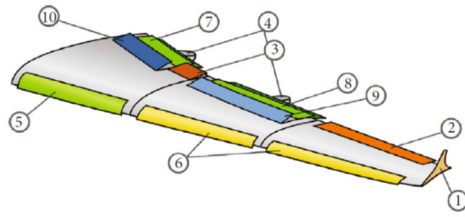


Figure 01. A conventional wing with control surfaces [19] (1) winglet, (2), (3) low/high-speed, (4) flap track fairing, (5) Kruger flaps, (6) slats, (7), (8) 3-slotted inner/outer flaps, (9) spoilers, and (10) spoilers-air brakes.

Among various types of morphing, the kinds of morphing are typically classified into three categories: in-plane morphing, airfoil morphing, and out-of-plane morphing [5, 20-22] as depicted in Fig. 02 (a). First, in-plane morphing refers to any changes in the wing configuration in the x and y plane: span, chord, and sweep; while airfoil morphing relates to changes in the airfoil shape: change in the camber's curve rate and thickness; lastly, out-of-plane types cover changes in the vertical direction, z: the spanwise bending and twist. This paper focuses on fine-scale airfoil changes, specifically the change in camber rate, referred to as camber morphing [23]. Camber is an airfoil's curvature, convexity, or asymmetry between the leading and trailing edges. Varying the camber rate has benefits in terms of control, lift distribution and airframe noise [23-26] as shown in Fig. 02 (b).

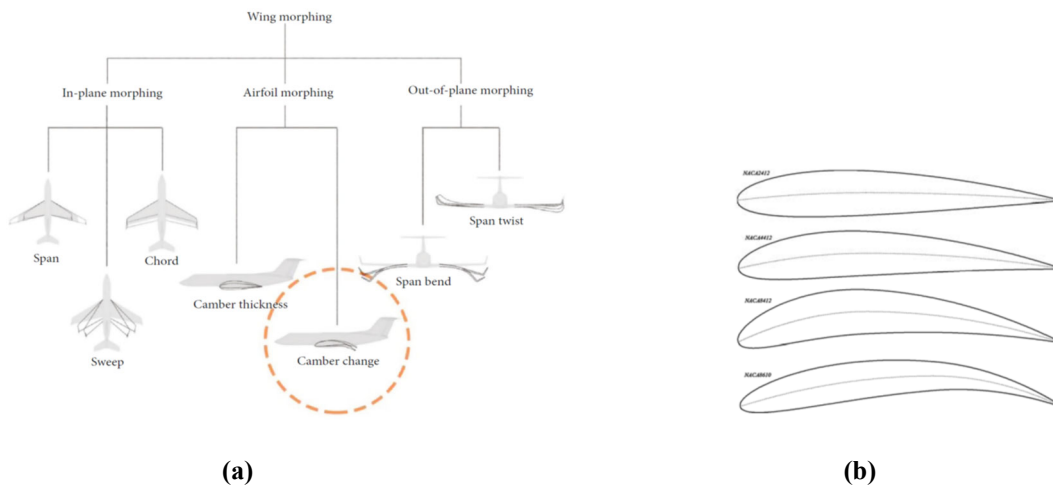


Figure 02. (a) Various types of morphing and (b) an exemplary picture of camber morphing profiles and their corresponding NACA profiles: NACA2412, 4412, 8412, and 8610.

Table 1 compares fixed-wing and morphing-wing aircraft in terms of their flight motion control methodologies, features, and key advantages and disadvantages. The significant advantage of using a morphing wing instead of a conventional fixed-wing aircraft is reduced D, resulting in enhanced range and sustainability. Additionally, reduced noise and improved radar signatures are also expected. Currently, the main reasons for passengers not adopting morphing wings in commercial aircraft are manufacturability, processing cost, and material strength [10-12, 18, 19, 27]. Designing, implementing, and controlling a camber-morphing wing in an aircraft for wind tunnel or flight testing is a challenging task. The internal structure for morphing is expected to be rigid and firm enough to maintain the morphed shapes and sustain structural deformation under the forces and stresses from multiaxial aerodynamic loadings while being flexible enough to deform in morphing directions. Thus, the design, implementation, and control of morphing wings require a comprehensive investigation of the morphing mechanisms, both mechanically and materially, as well as the actual manufacturability and practical implementation corresponding to flight—the cause and effects of morphing in flight. Therefore, this paper proposes a simple and effective design for morphing mechanisms that can be directly applied to UAVs.

Distinctive design parameters must be considered when designing a morphing mechanism, utilizing advanced materials, design strategies, and optimization techniques to achieve optimal performance. The optimization tools used,

as classified by Li and others [28], include topology optimization algorithms, parameter optimization, and evolutionary optimization, which are among the tools frequently employed in topology optimization to design camber morphing mechanisms. The objective function to be minimized can be structural weight, energy for shape reconfiguration, control authority, or aerodynamic characteristics. At the same time, the design variables include shape variables (such as the control points on the airfoil's boundary) and structural variables (such as the location of actuators). Based on the mechanism's synthesis method, tools used, and conceptual design, there are three categories: (1) structure-based, (2) material-based, and (3) hybrid. The classification is based on how shape morphing is conceptualized and physically implemented, whether it involves the internal structural layout, material characteristics, or a combination of both—a hybrid—that plays a significant role in morphing the wing [29]. This paper employs structure-based morphing mechanisms, focusing on a simple and effective design approach.

Table 1. Comparison between a fixed wing and a morphing wing aircraft

	Fixed Wing Aircraft	Morphing Wing Aircraft
Morphing Devices or Mechanisms	Control Surfaces: slats, slotted flaps, winglets, retractable landing gear [17]	Leading-Edge (LE) Trailing-Edge (TE) Global (LE+TE)
Features	Discrete, hinged, jointed	Continuous, flexible, elastic, jointless
Cons	- More D [30] - Flow separation - Airframe noise [31]	- Weight or complexity - Power consumption - Practicality of smart materials - Low-speed flight - Mostly applied to small aircraft
Pros	- Reliability - functionality	- Minimized flow separation - Improved L/D - Increased range [32] - Reduced fuel consumption - Reduced airframe noise [33] - D minimization [34] - Expanded operational envelope - Multi-functional

In summary, the authors of this paper developed a UAV with continuous, flexible, and elastic global morphing, featuring leading-edge and trailing-edge morphing, as well as jointless mechanisms in the main wing part. The tail section features elevators, a vertical stabilizer, and a rudder for yaw control.

Problem Statement

In most works of morphing UAV research, computational analysis and validation of outperforming aerodynamic performance are the primary concerns rather than the actual measurement of flight performance. Furthermore, most designs employ partial morphing, either at the trailing or leading edge, which reveals less aerodynamic improvement than conformal ones. Therefore, it is of interest to design, build, and fly camber morphing wing UAVs and validate their efficacy for practical applications and uses in the real world. Therefore, the significant problems with existing morphing wing designs and obstacles to overcome are as follows as an extended work of previously published paper by authors [35]:

A. Implementation of effective and conformal camber morphing mechanism

Unlike ground vehicles, aircraft have limited payloads and are still expected to maximize their endurance and flight ranges. Among various approaches to overcoming this limitation in UAVs, this paper addresses the problem of adopting conformal morphing in the airfoil, which substantially alters the L and D. However, its readiness at the flight-test stage and even the actual implementation of effective morphing mechanisms are far from being adopted in real-world usage. Considering the actual implementation of morphing mechanisms that change the curvature of the camber

using an actuator, it is crucial to design lightweight morphing on both leading and trailing edges, a smooth contour in the shape outline, and ease of manufacture.

B. Flight test of an aircraft with enhanced range and endurance

As mentioned earlier, most new design works on aircraft, especially for morphing UAVs, are currently limited to aerodynamic analysis and numerical validation using tools such as ANSYS or similar software. However, one of the primary purposes of UAVs is their task-driven maneuverability and agility, which must be practically validated through not only computational analysis but also flight tests in terms of performance, such as endurance, flight range, and trajectory and path planning related to control moments, roll, pitch, and yaw. The goal is to develop a highly sustainable aircraft for various commercial and military applications and validate its performance through flight tests.

Literature Survey

Most morphing-related works are limited in scope, particularly in terms of implementing the morphing mechanism and its computational analysis of aerodynamic performance. In other words, only a few works successfully implemented and tested flights. This literature review is limited to morphing aircraft up to the flight-level stage of development. There are three significant developments within the scope. First, Bilgen et al. [36] developed and successfully flight-tested an unmanned aircraft utilizing Macro-Fiber Composite actuators for solid-state control surfaces and effective roll control without traditional mechanical components. Their proposed morphing technique is shown in Fig. 03.

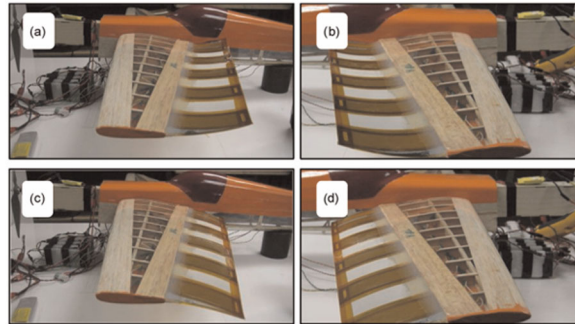


Figure 03. Left-wing: (a) peak negative actuation and (c) peak positive actuation. Right-wing: (b) peak negative and (d) positive actuation [36].

In this work, the researchers used NACA symmetrical airfoils as leading edge blended with thin trailing edge for morphing as well as tail stabilizer morphing using piezoelectric solid-state actuators. Fig. 04 shows the complete final design of the morphing aircraft and the UAVs during the flight. While theoretical analysis showed that the lift curve slope, drag polar, etc., were better for the morphing UAVs, wind tunnel test data showed that the steady-state roll rate of the morphing UAV was significantly lower than the baseline UAV due to the increase in the inertia of the morphing UAV.

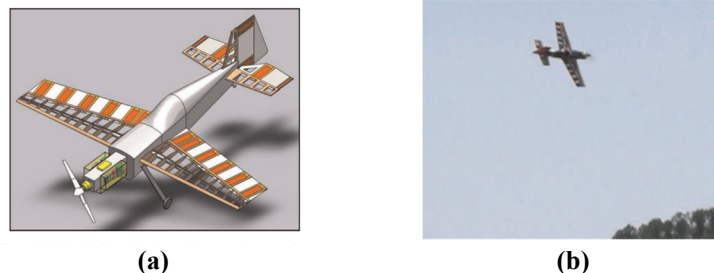


Figure 04. (a) Model of the final design of the morphing UAV and (b) actual morphing UAV in flight [36].

On the other hand, Chanzy and Keane [37] conducted a comprehensive study on morphing UAV wings, encompassing design, analysis, and experimental validation, to assess their aerodynamic performance and structural integrity. They employed a morphing wing technique featuring a flexible skin and variable camber mechanism,

optimized for improved aerodynamic performance and validated through wind tunnel testing. Their proposed model and actual wing are shown in Fig. 05.

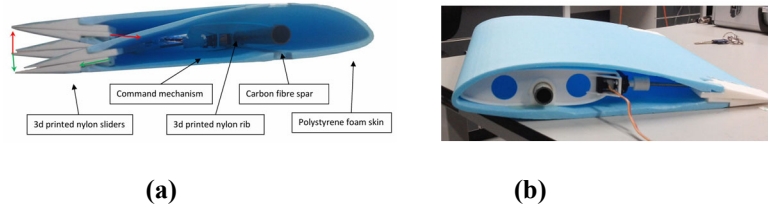


Figure 05. (a) 3D model of the morphing and (b) servo actuator with the sliding skin in the test section [37].

The researchers utilized servo actuators linked to a sliding mechanism to perform trailing-edge morphing. Another innovative idea proposed in this research is the sliding mechanism at the trailing edge, which was implemented using foam-made skin and a nylon-made slider. The actual flight test for the UAV with morphing wing and conventional wing is shown in Fig. 06.

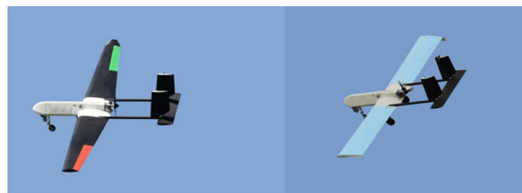


Figure 06. UAV flying with conventional wings (left) and morphing wings (right) [37]

As there was no hinge on the upper or lower surface of the wing, the proposed wing significantly reduced D. This leads to higher aerodynamic efficiency (L/D) in the case of morphing UAVs compared to conventional ones despite the lift force not experiencing a significant enhancement. On the contrary, in both flight tests and wind tunnel tests, it was found that the bank angle of the morphing UAV was less than that of the conventional ones. The morphing wing UAV had a 32% reduced roll rate compared to the traditional ones of the same dimension.

Last, Ozbek et al. [38] introduced the concept of the Rear Spar Articulated Wing Camber (RSAWC), a cost-effective morphing wing design for UAVs that enhances flight endurance by approximately 19% through a fishbone-like rib structure with rear spar articulation. Their RSAWC wing concept is shown in Fig. 07.



Figure 07. RSAWC concept wing test [38]

The researchers in this paper utilized fishbone-like 3D-printed wing ribs, known as the FishBac mechanism, as the basis for morphing wings. Servo motors were also connected to the wing to perform the morphing motion, and then a thermoplastic covering was used as the wing's surface. Several tests were performed, including desktop, wind tunnel, and actual flight tests. Fig. 08 (a) shows the developed RSAWC wing, and Fig. 08 (b) shows the UAVs in actual flight tests.



Figure 08. (a) RSAWC wing with covering, and (b) UAV with RSAWC wing during flight test [38]

The tests revealed that the morphing wing is more efficient, offering better aerodynamic performance and endurance. However, the proposed design in this study only includes trailing edge morphing rather than a complete camber morphing mechanism. All three examples mentioned above proposed innovative design approaches for the camber morphing of the wings. However, they only focused on trailing-edge morphing and experienced a lower roll rate than conventional base UAVs while having significantly better aerodynamic efficiency. A full-camber morphing mechanism, encompassing both leading-edge morphing and trailing-edge morphing, has the potential to deliver superior performance due to its ability to optimize the entire aerodynamic profile dynamically. This results in tighter turning radii, improved maneuverability, and a significantly broader flight envelope compared to partial morphing. The authors of this research have designed, implemented, and tested a novel and straightforward mechanism for combining the leading-edge and trailing-edge camber morphing of the wing, which is the primary contribution of this paper.

Design

Designing a conformal camber-morphing wing requires a thorough and calculative analysis procedure. It is imperative to analyze the effect of such design modifications before building UAVs. This section discusses the core design philosophy of the proposed mechanisms of camber-morphing wings. The detailed procedure is followed during the analysis stage.

A. Morphing Mechanisms

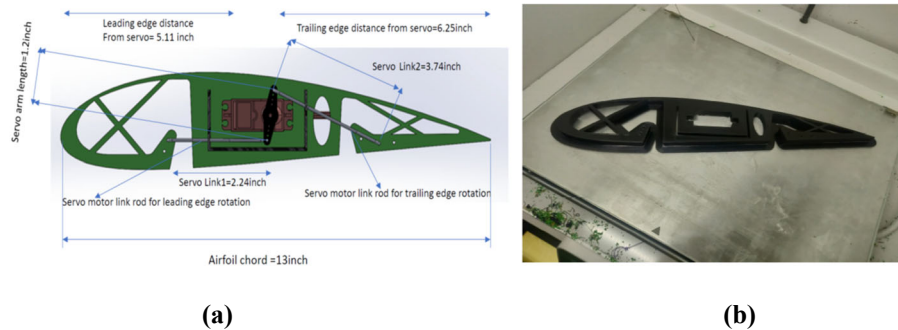


Figure 09. (a) CAD design of a camber morphing mechanism with detailed dimensions and (b) 3D-printed rib for the morphing mechanism where the Ultimaker 3D printer and PETG materials were used.

Fig. 09(a) shows a CAD model of the morphing mechanism designed using SolidWorks. A single servo motor drives it, and two servo link rods are attached to each side of the arm of the servo motor. When the motor rotates clockwise or counterclockwise, the rod pulls or pushes the flexible structure on both the leading and trailing edge parts, enabling conformal and smooth morphing across the entire airfoil surface area. Fig. 09 (a) also illustrates the detailed dimensions of the morphing mechanisms. Table 2 summarizes them.

Table 2. Detailed dimensions of the morphing mechanism in CAD models

Parts	Dimensions
Airfoil chord length	13 inches
Servo link length 1 (to the leading edge)	2.24 inches
Servo link length 2 (to the trailing edge)	3.74 inches
Servo arm length	1.2 inches
Leading edge distance from servo	5.11 inches
Trailing edge distance from servo	6.25 inches

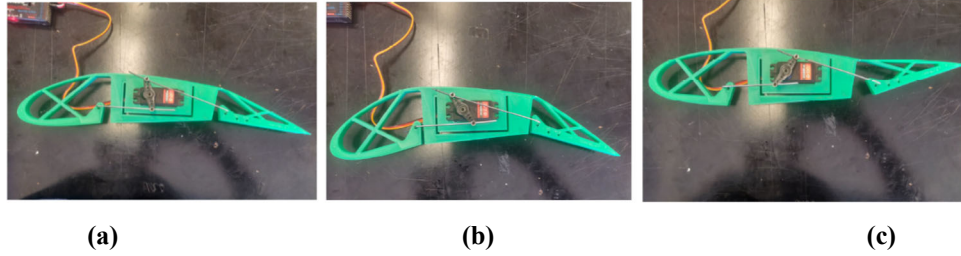


Figure 10. Three different morphing motions: (a) slightly positive, (b) full positive, and (c) negative morphing motions, respectively.

Fig. 10 shows various morphing-rated motions driven by the servo motor in the mechanism. The motor can rotate clockwise (CW) or counterclockwise (CCW). CW rotation creates a negative camber, and CCW rotation creates a positive camber as a function of the rotating angles.

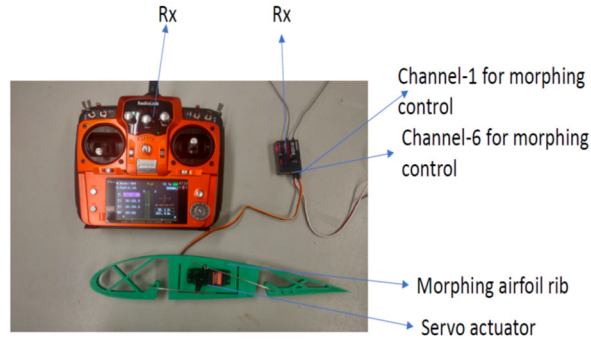


Figure 11. Electronic components for the camber motion control.

Fig. 11 illustrates the major RC electronics for variable camber motion control, including a manual transmitter (TX), a 12-channel receiver (RX), and related wiring configurations. A remotely controlled TX and RX have been adopted to verify the motions against CAD-designed models for conformal morphing. This simple and effective camber morphing mechanism is ideal for UAVs, which don't require highly sustainable structural strength from morphing and aerodynamic forces due to their slow operational speeds.

B. Kinematic Analysis

This section provides kinematic explanations of variable camber morphing intended to supplement aerodynamic and performance evaluations for full-scale UAV design and operations.

Morphing Characteristics

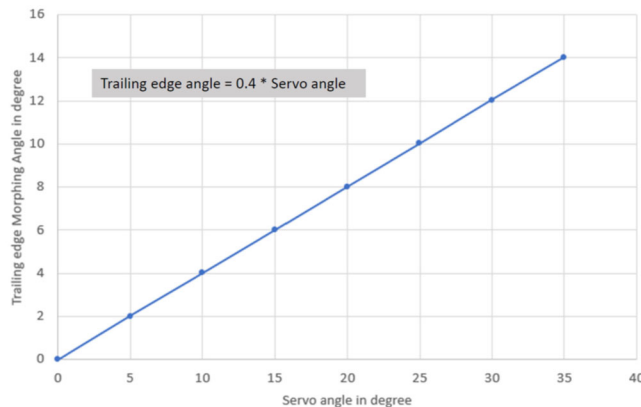


Figure 12. Morphed angles in the trailing edge vs. driven angles in the servo motor.

Fig. 12 visualizes the geometrical and physical morphed angles in the airfoil's trailing edge while the servo motor's angles are driven by control. The graph shows a linearly and monotonically increasing relation between them. The maximum angle from the servo is 35 degrees, and the corresponding angle on the trailing edge is 14 degrees—every 5 deg. In the servo, there are two degrees on the trailing edge. In an analytical form, the relation is described as follows in Eqn. (1).

$$\theta_{te} = 0.4 \cdot \theta_s \quad (1)$$

where θ_{te} is the angle of the trailing edge and θ_s is the angle of the servo motor arm.

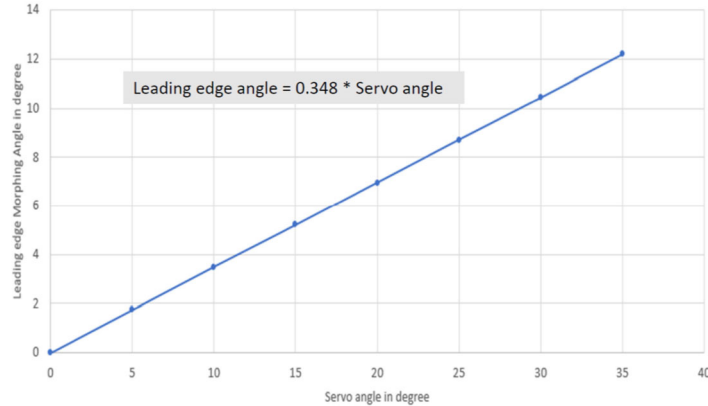


Figure 13. Morphed angles in the servo motor's leading edge vs. driven angles.

Like Fig. 12 above, Fig. 13 illustrates the geometrical and physical morphed angles at the airfoil's leading edge, where the servo motor's angles are controlled. The graph shows a linearly and monotonically increasing relation between them. Unlike the trailing edge, the maximum angle from the servo is 35 degrees, and the corresponding angle on the leading edge is 12 degrees, which is 2 degrees off compared to the trailing edge. As shown in Eqn. (2) every 5 degrees in the servo is less than 2 degrees (about 1.8~1.9) in the leading edge.

$$\theta_{le} = 0.348 \cdot \theta_s \quad (2)$$

where θ_{le} is the angle of the leading edge in the airfoil and θ_s is the angle of the servo motor arm.

C. Numerical Analysis of Performance Evaluation

This section describes the actual aerodynamical benefits of having camber morphing compared to conventional wings with deflection angles in the flaps. To evaluate its effectiveness, the author in this paper has two strategies: 1) to find L-matching cases, and 2) to compare D, which indicates L/D improvement that rigorously shows the expected and improved range and endurance when camber morphing wings are adopted to an actual UAV. The designed and implemented airfoil is the NACA 4412. The airfoil geometry imported into the Design Modeler was created using the CAD design software SolidWorks, based on the airfoil coordinates generated using a NACA 4-digit airfoil calculator. Fig. 14 shows the geometry of a morphing and a conventional airfoil with the indicated baseline (dotted line).

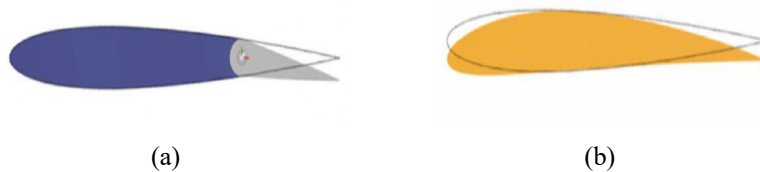


Figure 14. A schematic diagram of (a) a conventional airfoil with a deflection flap (purple) and (b) a morphing airfoil (yellow)

The designed and implemented airfoil is the NACA 4412. To find matching cases, the series of airfoil NACA \times 412 run cases such as 1412, 2412, through 9412 for the morphing airfoil cases, as shown in Fig. 15. For the conventional airfoil case, the flap joint was placed at 70% of the chord length of the NACA0012 airfoil, and the angle was rotated clockwise at the joint for the flap deflection angle. The camber rate changes from 0% to 9% in increments of 1%,

generating the morphing airfoil configurations, and the flap deflection angle varies in increments of 0.25 degrees. From 0 to 21.5 to generate deflecting airfoil configurations as depicted in Fig. 16.

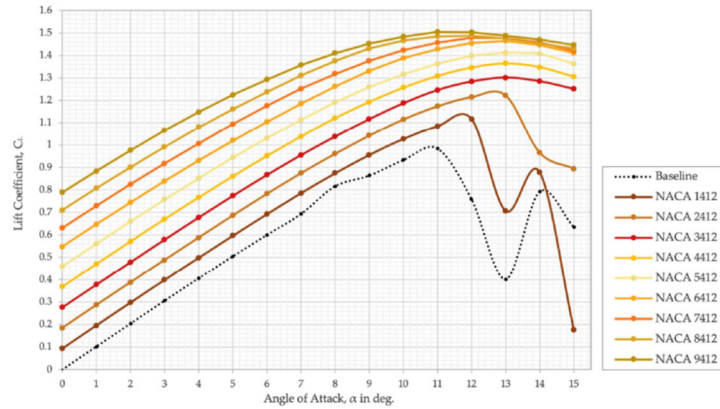


Figure 15. Morphing airfoil C_L vs. AoA varying the maximum camber rate.

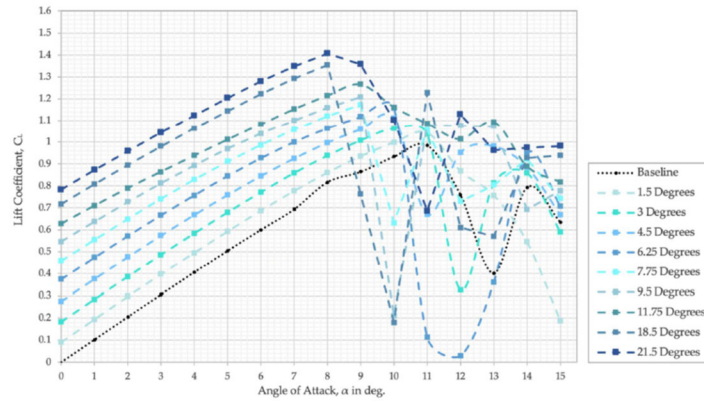


Figure 16. Conventional airfoil C_L vs. AoA varying the flap deflection angle.

Table 3. Summary of the matching cases

Matching cases	Morphing Airfoils	Conventional Airfoils
	Camber rate (%)	Deflection Angle (°)
Baseline	NACA 0012 – 0%	0°
Case 1	NACA 1412 – 1%	1.5°
Case 2	NACA 2412 – 2%	3°
Case 3	NACA 3412 – 3%	4.5°
Case 4	NACA 4412 – 4%	6.25°
Case 5	NACA 5412 – 5%	7.75°
Case 6	NACA 6412 – 6%	9.5°
Case 7	NACA 7412 – 7%	11.75°
Case 8	NACA 8412 – 8%	18.5°
Case 9	NACA 9412 – 9%	21.5°

Table 3 summarizes the results of the matching cases. Among matching cases between morphing and conventional wing configurations, the baseline wing configuration used in this paper is the NACA 4412 (4% camber morphing), corresponding to a 6.25° flap deflection.

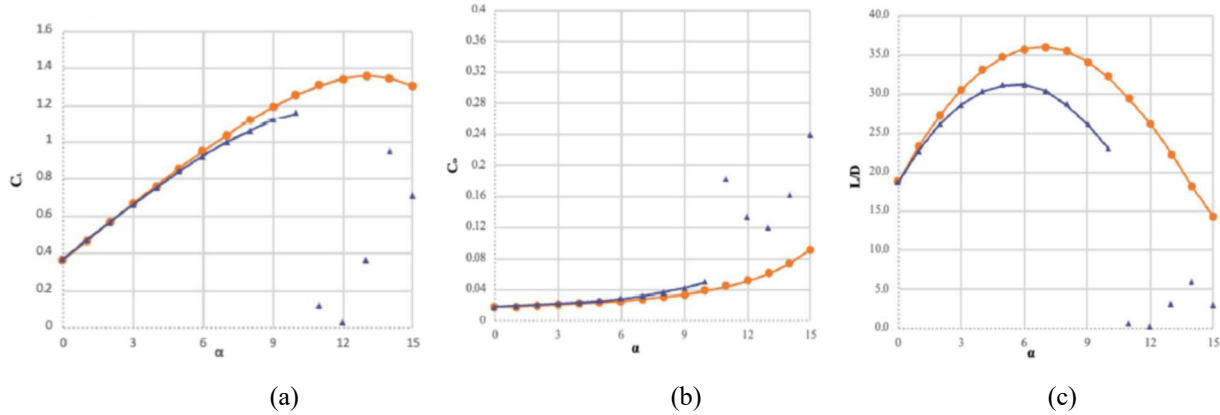


Figure 17. (a) C_L (b) C_D and (c) L/D vs. AoA each where conventional airfoil Lift coefficient (purple) vs. camber morphing (orange)

For these matching L morphing and conventional airfoils, D values were also computed and compared. Fig. 17 (a) depicts the lift coefficient (C_L) of both traditional and morphing cases. As AoA varies, it is observed that the graphs begin to separate after approximately 5-6 degrees of AoA. Meanwhile, Fig. 17 (b) and (c) describe the drag coefficient (C_D) comparison and L/D , respectively. While graphs are aligned with each other, in other words, when the Lift coefficient is matched while the AoA is changing from 0 to 5 deg., the L/D is improved from a minimum of 0 to a maximum of 12%. The aerodynamic parameter of interest was L/D or C_L/C_D ratios, which is used synonymously with aerodynamic performance in aeronautics. L/D or C_L/C_D measures the aerodynamic cruising efficiency, which can affect fuel consumption, range, and endurance, among other factors. The Breguet range equation is written as in Eqn. (3):

$$R = \left(\frac{v}{c}\right) \left(\frac{L}{D}\right) \ln\left(\frac{W_i + W_{fuel}}{W_i}\right) \quad (3)$$

where R is the cruise segment range, v is the constant cruise speed, W_{fuel} is the fuel weight, W_i is the fixed weight of the aircraft, and c is the thrust-specific fuel consumption for specific operating conditions. When taking other terms in Eqn. 5 to be constant, the maximum range can be achieved by maximizing the quantity C_L/C_D . In a particular cruise operation, a UAV's morphing wing can increase its range by 12%.

A 12% rise in the aircraft range makes studying the complete camber morphing mechanism significant. The thorough analysis procedure, encompassing both kinematic and numerical analysis, justifies the design of the camber morphing proposed and developed by the authors.

Implementation

Building the UAV is a considerable challenge, as it involves designing the rib for the morphing mechanism, assembling the wing with the ribs, and including all the control apparatus. Below are some crucial stages in the building process.

A. Wing Construction

The wing structure was fabricated using carbon fiber for its high strength-to-weight ratio and stiffness. Each wing incorporated three servo motors dedicated to morphing. The leading and trailing edges of the airfoil could change camber dynamically, enabling precise roll control during flight. The completed wings underwent morphing tests, ensuring smooth transitions and robust performance under simulated flight loads. A 3D design of the wing and the ribs is shown in Fig. 18 (a). Additionally, the difference in morphing between the two sides of the wing during a rightward rolling condition is shown in Figs—18 (b) and (c).

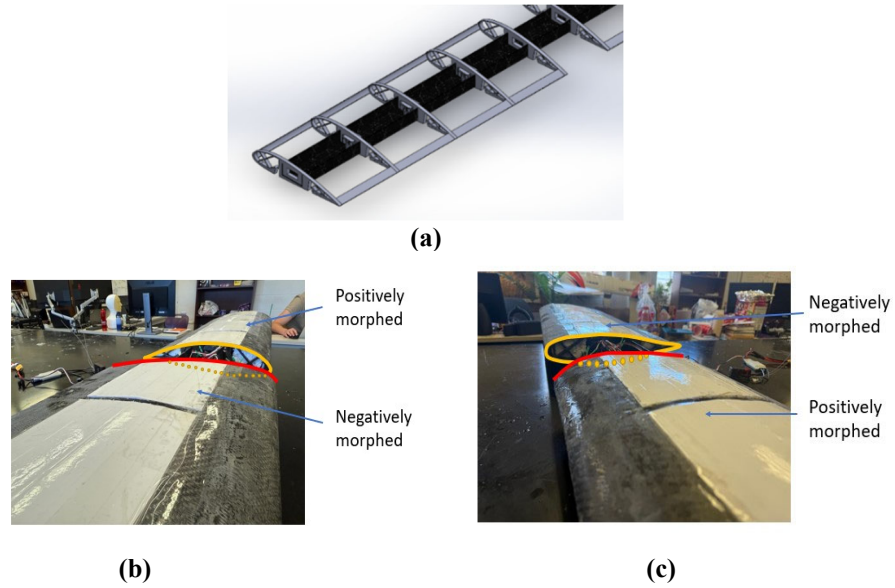


Figure 18. (a) 3D CAD design of the wing for conformal camber morphing wing, morphing for rightward rolling for (b) the left wing and (c) the right wing, where positive (yellow) and negative morphing (red) accordingly.

B. Fuselage and Tail Design

The fuselage and tail assembly were also modeled in SolidWorks, with a focus on aerodynamics, weight distribution, and structural compatibility with the wings. The fuselage was constructed from lightweight carbon fiber composite and Styrofoam to house the avionics and battery, ensuring a total weight of 8.1 kg for the UAV. The motor is mounted in front of the fuselage for the propulsion of the UAV, and a solid wooden block is used to mount the motor. The fuselage features two canopies: a front or nose canopy and a rear canopy. The nose canopy creates the opening to install the battery, ESC, and other components in proper locations inside the fuselage. The rear canopy is used during the assembly of the wing on the fuselage and when connecting the tail servo cables to the receiver. It perfectly fixes the wing with the fuselage and tail wiring. The front landing gear is mounted on the bottom surface of the fuselage, and the tail wheel is mounted at the end of the tail boom, integrated with a servo motor to ensure steering during the ground run for takeoff. Fig. 19 shows the different structural components of the UAV.

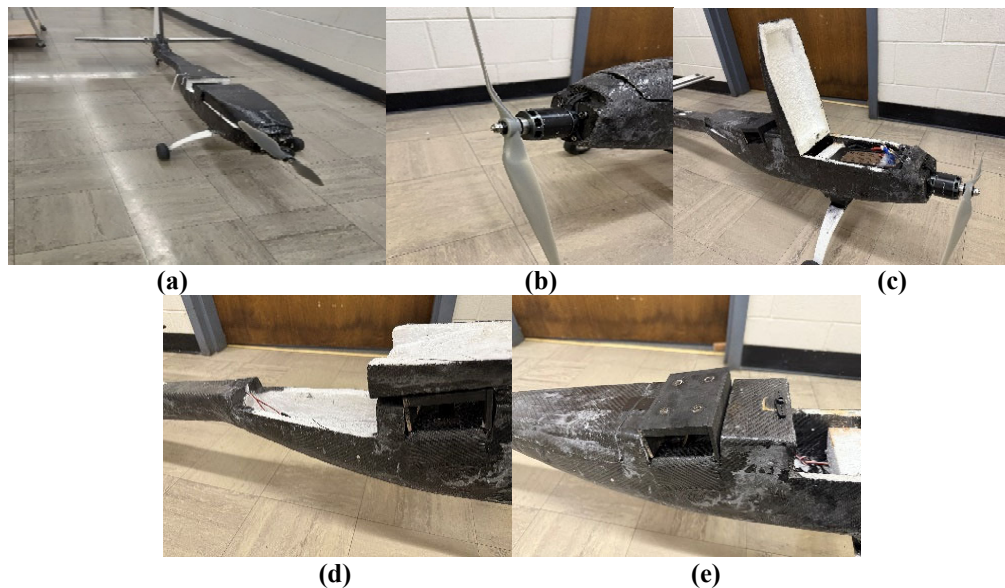


Figure 19. (a) The fuselage of the UAV, (b) motor mounting, (c) nose canopy, (d) rear canopy, and (e) wing mounting

A conventional tail ensures the UAV's static and directional stability in flight. The horizontal stabilizer is mounted on the tail boom, extending up the main wing to provide a wake that does not significantly affect the tail, thereby achieving higher efficiency. Two independent servo motors actuate horizontal and vertical stabilizers. Fig. 20 shows the horizontal and vertical stabilizers mounted on the tail boom.



Figure 20. Horizontal and vertical stabilizers

C. Assembly and Integration

All components, including the wings, fuselage, and tail, were assembled precisely. Servo motors were synchronized with a flight control system to manage roll control via morphing. This eliminated the need for traditional ailerons, providing smoother control inputs. The wing is fastened to the fuselage using four bolts and nuts to support the UAV's overall weight, as well as its vibration and aerodynamic loads, in any circumstance, whether in flight or on the ground. Fig. 21 (a) shows the complete assembly of the UAV, while Fig. 21 (b) shows the assembled wing mounted on the fuselage without the skin.



Fig. 21 (a) Complete assembled and (b) without wing skin

Test Flight

The camber morphing flight test is carried out in multiple steps. The detailed approach for the flight is as follows: 1) ground tests: static and dynamic tests are performed to validate the morphing mechanism's responsiveness of the main wing, control responsiveness of other control surfaces such as the rudder and elevator, durability of the UAV, and power distribution and stability, 2) flight tests: controlled flight trials confirm that the morphed shapes and corresponding control moments are generated effectively and manages roll control and improves aerodynamic performance, and 3) performance metrics: key metrics such as roll rate, morphing actuation speed, and aerodynamic efficiency will be recorded and analyzed to refine the design. The flight test is performed at the Hyder-Burke Center of Tennessee Technological University (TTU), as shown in Fig. 22(a).

The performance from the flight test, as shown in Figs. 22(b)-(c) is primarily focused on the mission-planned flight, utilizing rolling moment control from the main morphing wings. Conventional control surfaces in the airplane handle other control moments, such as pitch and yaw moments, to remove any unexpected adverse yaw.

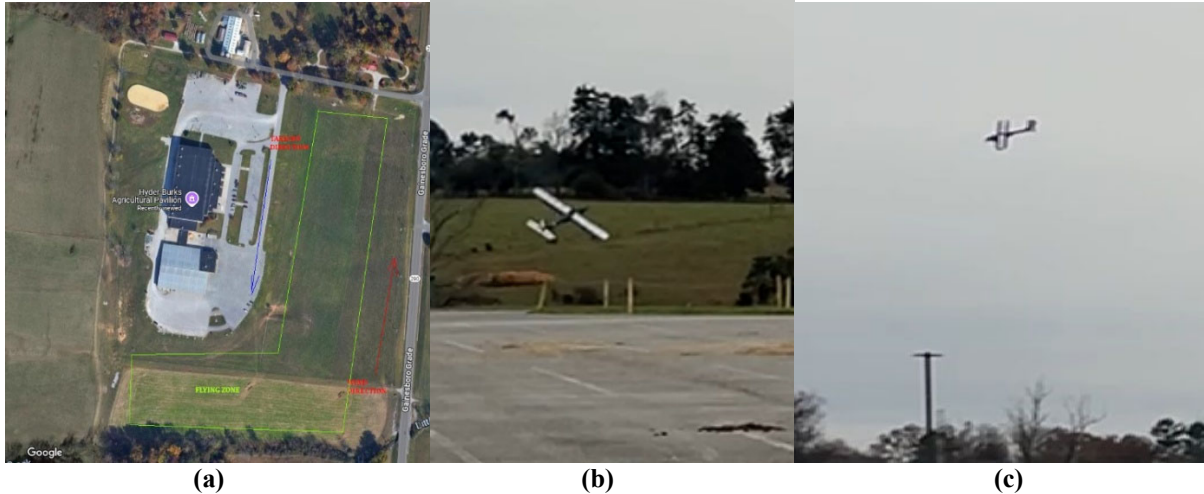


Figure 22. (a) Hyder-Burke Center at Tennessee Tech University (TTU) for the flight test, (b)-(c) flight test scenes

Summary

The authors have successfully designed a new concept of conformal camber morphing airfoil ribs and implemented a morphing mechanism using servo motor actuators. Extensive design considerations have been taken into account for the initial design of the UAV. Unlike other existing morphing airplanes that partially morph at the trailing or leading edge, the authors of this paper successfully designed a global or conformal camber morphing UAV and conducted test flights. Later, different aerodynamic equations are used to evaluate the operating parameter at selected cruise conditions considering the power of the chosen propulsion system. Table 4 provides detailed parameters of the UAV, including design parameters such as total weight, wing area, fuselage length, and propeller thrust, as well as operating parameters like cruise speed, altitude, and turning radius.

Table 4. Detailed parameters of the conformal camber morphing UAV

Description of parameters	Value
Airfoil profile	NACA 4418
Total weight, W	8.1 kg
Wingspan, b	2.225 m
Wing chord, c	0.325 m
Length of fuselage	1.7 m
Height	0.63 m
Wing area	0.7 m ²
Horizontal stabilizer area	0.15m ²
Vertical stabilizer area	0.056 m ²
Wing loading	11.57 kg/m ²
Cruise speed @ 2000 ft altitude	15.45 m/s
Reynolds number	302194.1841
Total motor power p	1800 W
Propeller diameter	0.45 m
ESC rating	120 Amp
Lift coefficient, C _L	0.97
Li-Po battery rating	12,000 mAh, Voltage 22.2 V
Morphing servo rating	40 Kg-cm torque
Turning radius@16.6m/s	55.45m
Banking angle ϕ	27.76 ^o

Significance and Conclusion

This project detailed the design, development, and testing of a UAV featuring leading and trailing-edge camber morphing for roll control. The airfoil morphing system utilized a compliant rib structure designed in SolidWorks and fabricated using 3D printing. Equally spaced, three servo motors were integrated into each wing to actuate the morphing mechanism simultaneously. The wings, fuselage, and tail were constructed primarily from carbon fiber, ensuring lightweight and durable components for a total UAV weight of 8.1 kg. This innovative morphing system replaced traditional ailerons, providing precise aerodynamic control. Extensive testing, including ground and flight trials, validated the system's functionality and performance improvements. These camber-morphing wing UAVs are expected to exhibit comprehensive and enhanced performance in various aspects, including radar signature, noise profile, portability, repairability, on-demand design alterations, and overall aerodynamic performance. In addition, the successful development of this camber-morphing UAV demonstrates the feasibility and effectiveness of adaptive airfoil technologies to enhance other types of UAVs in the future. The compliant morphing mechanism could deliver efficient roll control while maintaining structural integrity and aerodynamic efficiency. Additionally, although all actuators are controlled simultaneously in this paper, later, each actuator is controlled separately to generate various flight motions. From a manufacturing perspective, by leveraging advanced materials such as carbon fiber and integrating modern design tools and manufacturing techniques, the project showcases the potential of morphing technology to enhance the maneuverability and multi-role capabilities of UAVs. Future developments could focus on scalability, further optimization of the morphing mechanism, and expanding its applications across different platforms.

Acknowledgement of Support and Disclaimer

This material is based upon work supported by the National Aeronautics and Space Administration under Grant No. 80NSSC23M0060 issued through the University Leadership Initiative Program. Any opinions, findings, conclusions, or recommendations expressed in this material are those of the author(s) and do not necessarily reflect the views of NASA. Additionally, this research is partially supported by Tennessee Technological University's URECA and CISE funding for the 2023-2024 period. The authors greatly appreciate Ms. T. Majid at ETHZ for her foundational work.

References

1. Bishop, C., et al., *What is metamorphosis?* Integrative and Comparative Biology, 2006. **46**(6): p. 655-661.
2. Dodd, M. and J. Dodd, *The biology of metamorphosis*. Physiology of the Amphibia, 1976. **3**(2): p. 467-599.
3. Harvey, C., et al., *A review of avian-inspired morphing for UAV flight control*. Progress in Aerospace Sciences, 2022. **132**: p. 100825.
4. Truman, J.W. and L.M. Riddiford, *The origins of insect metamorphosis*. Nature, 1999. **401**(6752): p. 447-452.
5. Sofla, A., et al., *Shape morphing of aircraft wing: Status and challenges*. Materials & Design, 2010. **31**(3): p. 1284-1292.
6. Barbarino, S., et al., *A review of morphing aircraft*. Journal of intelligent material systems and structures, 2011. **22**(9): p. 823-877.
7. Kim, T., S. Siddiqui, and B. Jo. *Estimation of Critical Aeroelastic Damping Using Dynamic Eigen Decomposition and Artificial Damping*. in *AIAA AVIATION FORUM AND ASCEND 2024*. 2024.
8. Jo, B.W., et al. *Towards the Conversion to Electrified Commercial Aircraft, the Boeing 737 Max 800 Field Data Analysis*. in *AIAA AVIATION FORUM AND ASCEND 2024*. 2024.
9. Saha, A.K., J. Femi-Oyetero, and B.W. Jo. *Flight Range Estimation of Boeing 737 Max, Commercial Aircraft With SOFC (Solid Oxide Fuel Cells) Propulsion Systems*. in *AIAA SCITECH 2025 Forum*. 2025.
10. Ameduri, S. and A. Concilio, *Morphing wings review: Aims, challenges, and current open issues of a technology*. Proceedings of the Institution of Mechanical Engineers, Part C: Journal of Mechanical Engineering Science, 2023. **237**(18): p. 4112-4130.
11. Guo, J., C. Zhao, and Z. Song. *Discussion on research status and key technologies of morphing aircraft*. in *Journal of Physics: Conference Series*. 2022. IOP Publishing.
12. Jha, A.K. and J.N. Kudva. *Morphing aircraft concepts, classifications, and challenges*. in *Smart structures and materials 2004: industrial and commercial applications of smart structures technologies*. 2004. SPIE.
13. Reich, G. and B. Sanders, *Introduction to morphing aircraft research*. Journal of aircraft, 2007. **44**(4): p. 1059-1059.
14. Rodriguez, A. *Morphing aircraft technology survey*. in *45th AIAA aerospace sciences meeting and exhibit*. 2007.

15. TSUSHIMA, N. and M. TAMAYAMA, *Recent researches on morphing aircraft technologies in Japan and other countries*. Mechanical Engineering Reviews, 2019. **6**(2): p. 19-00197-19-00197.
16. Weisshaar, T.A., *Morphing Aircraft Technology æ New Shapes for Aircraft Design*. 2006.
17. Weisshaar, T.A., *Morphing aircraft systems: historical perspectives and future challenges*. Journal of aircraft, 2013. **50**(2): p. 337-353.
18. Ajaj, R.M., C.S. Beaverstock, and M.I. Friswell, *Morphing aircraft: The need for a new design philosophy*. Aerospace Science and Technology, 2016. **49**: p. 154-166.
19. Somnic, J. and B.W. Jo, *Status and challenges in homogenization methods for lattice materials*. Materials, 2022. **15**(2): p. 605.
20. La, S., et al. *Surveys on skin design for morphing wing aircraft: status and challenges*. in *2018 AIAA aerospace sciences meeting*. 2018.
21. Alsaidi, B., W.Y. Joe, and M. Akbar, *Simplified 2D skin lattice models for multi-axial camber morphing wing aircraft*. Aerospace, 2019. **6**(8): p. 90.
22. Alsaidi, B., W.Y. Joe, and M. Akbar, *Computational analysis of 3D lattice structures for skin in real-scale camber morphing aircraft*. Aerospace, 2019. **6**(7): p. 79.
23. Jo, B.W. and T. Majid, *Aerodynamic analysis of camber morphing airfoils in transition via computational fluid dynamics*. Biomimetics, 2022. **7**(2): p. 52.
24. Jo, B.W. and T. Majid, *Enhanced range and endurance evaluation of a camber morphing wing aircraft*. Biomimetics, 2023. **8**(1): p. 34.
25. Alsulami, A., M. Akbar, and W.Y. Joe. *A comparative study: Aerodynamics of morphed airfoils using CFD techniques and analytical tools*. in *ASME International Mechanical Engineering Congress and Exposition*. 2017. American Society of Mechanical Engineers.
26. Majid, T. and B.W. Jo, *Comparative aerodynamic performance analysis of camber morphing and conventional airfoils*. Applied Sciences, 2021. **11**(22): p. 10663.
27. Somnic, J. and B.W. Jo, *Homogenization methods of lattice materials*. Encyclopedia, 2022. **2**(2): p. 1091-1102.
28. Li, D., et al., *A review of modelling and analysis of morphing wings*. Progress in Aerospace Sciences, 2018. **100**: p. 46-62.
29. Majid, T. and B.W. Jo, *Status and challenges on design and implementation of camber morphing mechanisms*. International Journal of Aerospace Engineering, 2021. **2021**(1): p. 6399937.
30. Nguyen, N.T., et al. *Wind tunnel investigation of a flexible wing high-lift configuration with a variable camber continuous trailing edge flap design*. in *33rd AIAA Applied Aerodynamics Conference*. 2015.
31. Dobrzynski, W., *Almost 40 years of airframe noise research: what did we achieve?* Journal of aircraft, 2010. **47**(2): p. 353-367.
32. Kota, S., et al. *Mission adaptive compliant wing–design, fabrication and flight test*. in *RTO Applied Vehicle Technology Panel (AVT) Symposium*. 2009. RTO-MP-AVT-168, Evora, Portugal.
33. Arena, M., et al., *Flutter clearance investigation of camber-morphing aileron tailored for a regional aircraft*. Journal of Aerospace Engineering, 2019. **32**(2): p. 04018146.
34. Nguyen, N., et al. *Development of variable camber continuous trailing edge flap for performance adaptive aeroelastic wing*. in *SAE AeroTech Congress & Exhibition*. 2015.
35. Islam, M.A., et al. *Design and Implementation of a Variable Camber Mechanism for a Small Fixed-Wing UAV (Unmanned Aerial Vehicle)*. in *2024 IEEE International Conference on Robotics and Biomimetics (ROBIO)*. 2024. IEEE.
36. Bilgen, O., et al., *A novel unmanned aircraft with solid-state control surfaces: Analysis and flight demonstration*. Journal of Intelligent Material Systems and Structures, 2013. **24**(2): p. 147-167.
37. Chanzy, Q. and A. Keane, *Analysis and experimental validation of morphing UAV wings*. The Aeronautical Journal, 2018. **122**(1249): p. 390-408.
38. Ozbek, E., S. Ekici, and T.H. Karakoc, *Unleashing the Potential of Morphing Wings: A Novel Cost Effective Morphing Method for UAV Surfaces, Rear Spar Articulated Wing Camber*. Drones, 2023. **7**(6): p. 379.